Ecotoxicology and Environmental Safety 180 (2019) 168–178

Contents lists available at ScienceDirect

Ecotoxicology and Environmental Safety

journal homepage: www.elsevier.com/locate/ecoenv

Fluorene-9-bisphenol exposure induces cytotoxicity in mouse oocytes and causes ovarian damage

Zhenzhen Jia[a,d,1], Hongyu Wang[a,1], Zeyang Feng[b], Shaozhi Zhang[a], Lining Wang[a], Jingwen Zhang[a], Qianqian Liu[a], Xin Zhao[b,***], Daofu Feng[c,**], Xizeng Feng[a,*]

[a] State Key Laboratory of Medicinal Chemical Biology, The Key Laboratory of Bioactive Materials, Ministry of Education, College of Life Science, Nankai University, Tianjin, 300 071, China
[b] The Institute of Robotics and Automatic Information Systems, Nankai University, Tianjin, 300 071, China
[c] Department of General Surgery, Tianjin Medical University General Hospital, No. 154 Anshan Road, Tianjin, 300052, China
[d] College of Life Science, Shandong Normal University, Shandong Provincial Key Laboratory of Animal Resistance Biology, Institute of Biomedical Sciences, Key Laboratory of Food Nutrition and Safety of Shandong Normal University, Jinan, 250014, China

ARTICLE INFO

Keywords:
Endocrine-disrupting chemicals
BHPF
Oocyte maturation
Oxidative stress
Ovary damage

ABSTRACT

Fluorene-9-bisphenol (BHPF), a substitute for bisphenol A, is a chemical component of plastics for industrial production. There is evidence that BHPF exerts an antioestrogenic effect on mice, induces endometrial atrophy and leads to adverse pregnancy outcomes. However, the effects of BHPF on oocyte maturation and ovary development as well as its possible mechanisms remain unclear. The objective of this study was to investigate the toxicity and mechanism of BHPF exposure in mouse oocytes *in vitro* and *in vivo*. Our results showed that BHPF could inhibit the maturation of oocytes *in vitro* by reducing the protein level of p-MAPK and destroying the meiotic spindle. We found that *in vitro,* BHPF-treated oocytes showed increased ROS levels, DNA damage, mitochondrial dysfunction, and expression of apoptosis- and autophagy-related genes, such as Bax, cleaved-caspase 3, LC 3 and Atg 12. In addition, *in vivo* experiments showed that BHPF exposure could induce the expression of oxidative stress genes (Cat, Gpx 3 and Sod 2) and apoptosis genes (Bax, Bcl-2 and Cleaved-caspase 3) and increase the number of atresia follicles in the ovaries. Our data showed that BHPF exposure affected the first polar body extrusion of oocytes, increased oxidative stress, destroyed spindle assembly, caused DNA damage, altered mitochondrial membrane potentials, induced apoptosis and autophagy, and affected ovarian development.

1. Introduction

Endocrine-disrupting chemicals (EDCs) are chemical substances that interfere with human and animal reproduction and development (Patisaul and Adewale, 2009; Vandenberg et al., 2009). In recent years, bisphenol A (BPA) has been widely used in the manufacturing of polycarbonate plastic and epoxy resins and become one of the most extensively used EDCs (Ding et al., 2017; Geens et al., 2012). BPA was shown to exhibit oestrogenic activity and could affect preimplantation embryo development (Xiao et al., 2011), decrease fertility and fecundity (Cabaton et al., 2011), cause metabolic abnormalities (Susiarjo et al., 2015, 2017), and induce the apoptosis of germ cells (Wang et al., 2017). With the negative impact of BPA on reproduction and development, BPA substitutes are often used in industrial production. BHPF is a bisphenol compound containing a fluorenyl group that can be used as a substitute for BPA (Dai et al., 2009; Korshak et al., 1971; Liu et al., 2008; Wang and Zhang, 2015). Because of its exceptional heat resistance, high refractive index, high transparency and low linear coefficient of expansion (Dai et al., 2009), BHPF is commonly utilized in the synthesis of polyester polymers (Korshak et al., 1971). The thermal stability of fluorene epoxy resin was shown to be higher than that of BPA resin (Dai et al., 2009). As the fluorene content increases, the decomposition activation energy of the resin increases (BPA/4,4-(9-fluorenylidene)-dianiline (FDA) resin: 181.97 kJ/mol; BHPF/FDA resin: 249.40 kJ/mol) (Dai et al., 2009).

Previous research has shown that BHPF possesses antioestrogenic

* Corresponding author.
** Corresponding author.
*** Corresponding author.
E-mail addresses: author.zhaoxin@nankai.edu.cn (X. Zhao), jerryfenglc@sina.com (D. Feng), xzfeng@nankai.edu.cn (X. Feng).
[1] These authors contributed equally to this work.

https://doi.org/10.1016/j.ecoenv.2019.05.019
Received 20 March 2019; Received in revised form 27 April 2019; Accepted 7 May 2019

activity, which leads to atrophy of the endometrium and adverse effects on pregnancy in mice (Zhang et al., 2017). As a substitute for BPA, BHPF exerts a strong antioestrogenic effect, although it exerts no oestrogenic effect. With the popularization of BHPF, it is important to explore the effects of BHPF on oocyte maturation and development.

Oocyte maturation influences the quality of oocytes, which is critical for fertilization and embryonic development (Rizos et al., 2002). Several important factors, including oxidative stress, DNA damage, cell apoptosis and autophagy, exert a strong influence on the oocyte maturation process (Yue et al., 2016). Considerable evidence suggests that oxidative stress can damage DNA repair processes, cause meiotic segregation errors (Perkins et al., 2016), induce apoptosis and autophagy (Liu et al., 2015; Tang et al., 2015), and thus affect different biological processes.

We assumed that BHPF influences oocyte maturation by causing DNA damage, injuring the subcellular structure , and inducing oxidative stress, autophagy, apoptosis and ovarian damage. Therefore, we investigated the toxic effects of BHPF on mouse oocyte maturation progression and ovarian development as well as its possible mechanisms.

2. Materials and methods

2.1. Animals and reagents

All experimental procedures involving mice were approved by the Committee for Animal Experimentation of the College of Life Sciences at Nankai University (No. 2008) and performed in accordance with the NIH Guide for the Care and Use of Laboratory Animals (National Research Council, 2011). Female CD-1 mice (8-weeks old) and specific pathogen free (SPF) mouse food were obtained from the Institute of Zoology of the Chinese Academy of Sciences (Beijing, China). The mice were housed in cages at 22 ± 2 °C with proper light/dark cycles and fed a regular diet. The lights were turned on at 8 a.m. and turned off at 8 p.m. to maintain a 12/12 h light/dark cycle. The mice were allowed to adapt to the abovementioned experimental conditions for at least 7 days and then randomly divided into control and experimental groups.

BHPF was purchased from Sigma-Aldrich (Saint Louis, MO, USA, purity 97%, CAS: 3236-71-3). Pregnant mare serum gonadotropin (PMSG), human chorionic gonadotropin (hCG) and other chemicals used in the following experiments were obtained from the Ningbo Second Hormone Factory (China).

2.2. BHPF treatment

During the *in vitro* experiment, BHPF was dissolved in DMSO (Sigma-Aldrich, MO, Saint Louis, USA, purity ≥ 99.5%, CAS: 67-68-5) and then diluted with M16 medium (Sigma-Aldrich, MO, Saint Louis, USA, M7292) to concentrations of 50, 100, 200 and 400 μM (Ding et al., 2017; Jiao et al., 2019); the final concentration of DMSO in the culture medium was 0.1%. The control group was cultured under the same culture conditions with the same concentration of DMSO. At different time points after culturing, oocytes were collected for subsequent analysis.

During the *in vivo* experiment, BHPF was dissolved in peanut oil to the appropriate concentrations. Mice in the experimental groups were treated with BHPF (daily dose of 2, 10, 50 mg/kg of body weight (Zhang et al., 2017), administered by gastric cannula, once per day for 12 days, while mice in the control group were treated with the same volume of peanut oil in the same manner.

2.3. Oocyte collection and culture

During the *in vitro* experiment, superovulation was induced in the mice by intraperitoneal injection of 10 IU PMSG. Germinal vesicle stage oocytes from the ovary were further cultured in M16 medium containing 0.1% DMSO with or without BHPF to final concentrations of 50, 100, 200 and 400 μM. The oocytes were cultured with liquid paraffin oil in an incubator at 5% CO_2 and 37 °C. Then, after 14 h of culturing, the oocytes were collected for Western blot analysis (cell number: 150) and a separate series of immunofluorescence experiments.

During the *in vivo* experiment, the mice were superovulated by intraperitoneal injection of 10 IU PMSG followed by 10 IU hCG after 48 h. Approximately 14 h after the hCG injection, the mice were sacrificed via cervical dislocation, and metaphase II (MII) oocytes were collected from fallopian tube ampullae in M2 medium (Sigma-Aldrich, MO, Saint Louis, USA, M7167) after BHPF treatment (Meng et al., 2016).

2.4. Immunofluorescence and confocal microscopy

To determine the amount of ROS generation, oocytes were incubated with the oxidation-sensitive fluorescent probe 5-(and-6)-chloromethyl-2′, 7′-dichlorodihydrofluorescein diacetate (DCFH-DA, Solarbio Science & Technology Company, Beijing, China, CSA: 4091-99-0, 1 μM) for 30 min and washed twice in PBS buffer. Then, the fluorescence was detected using confocal microscopy (measured at 525 nm and excited at 488 nm), and the fluorescence intensity of each oocyte was analysed by ImageJ software.

For analyses of spindle morphology and chromosomal arrangement, oocytes were collected and fixed in PFA for 30 min. Then, the fixed samples were permeabilized in 0.5% Triton X-100 for 20 min at room temperature. After washing twice in PBS, the samples were incubated in PBS containing 1% BSA (block solution) for 1 h. Then, the oocytes were incubated with α-tubulin antibody (Cell Signaling Technology, Beverly, MA, USA, 3783S, mouse antibody), which was diluted 1:200 in blocking solution overnight at 4 °C in the dark. The anti-mouse IgG Fab2 fragment (Cell Signaling Technology, Beverly, MA, USA, 4408, 1:100 dilution) was added, and the mixture was incubated for 30 min in the dark at room temperature. Chromosomes were counterstained with 10 μg/ml DAPI for 5 min. Finally, the oocytes were observed by laser scanning confocal microscopy. The fluorescence intensity of each oocyte was analysed by ImageJ software.

To determine the amount of DNA damage, GV oocytes were cultured with IBMX (Beyotime Biotechnology Company, Shanghai, China, SC0195) and treated with100 μM BHPF for 8 h. The rabbit anti-γ-H2AX antibody (Cell Signaling Technology, Beverly, MA, USA, 9718S, 1:200 dilution) was used for immunofluorescence labelling to observe DNA double-strand breakage. Then, the oocytes were measured using a confocal microscope. At least 50 oocytes were analysed for each group. The fluorescence intensity of each oocyte was analysed by ImageJ software.

The oocyte mitochondrial membrane potential was determined by staining with the JC-1 probe (Beyotime Biotechnology Company, Shanghai, China, C2006) to evaluate oocyte mitochondrial function. Briefly, the oocytes were incubated with a JC-1 buffer solution supplemented with 10 μg/ml probes for 30 min. The oocytes were observed by laser scanning confocal microscopy, and the fluorescence intensity of the oocytes was analysed by ImageJ software.

To assess the levels of autophagy and apoptosis, oocytes were cultured with 100 μM BHPF, a mouse anti-annexin-V antibody (Santa Cruz Biotechnology, Santa Cruz, CA, sc-74438, 1:200) and a rabbit anti-LC3 antibody (Cell Signaling Technology, Beverly, MA, USA, 2775, 1:200 dilution) for 14 h and then observed by confocal microscopy. The fluorescence intensity of each oocyte was analysed by ImageJ software.

2.5. Analysis of ovary biopsy

The ovaries were immediately removed, fixed in paraformaldehyde solution and dehydrated in alcohol. Then, the ovaries were cleared in xylene and embedded in paraffin. The cortical region of each ovary was cut into serial sections (5 μm thick). The slices were stained with

haematoxylin and eosin, dehydrated with serial dilutions of alcohol and cleared in xylene. The corpora lutea and follicles of each ovary from each mouse were observed under a light microscope.

2.6. Western blot analysis

Approximately 200 mouse oocytes were collected at the MI stage, lysed in buffer (SDS sample buffer with 2-mercaptoethanol), heated at 100 °C for 5 min and immediately frozen at −20 °C until use. Protein was separated by SDS-polyacrylamide gel electrophoresis (PAGE) using 12% gels. After electrophoretic separation, proteins were electrically transferred to a PVDF membrane (Immobilon-P; Millipore, Bedford, MA), which was pretreated with methanol. To avoid nonspecific binding, the membranes were blocked in TBS (25 mM Tris, 150 mM NaCl, pH 8.0) containing 0.01% Tween-20 (TBST) and 5% BSA at room temperature for 1 h. After washing with TBST, the membrane was incubated overnight at 4 °C with the following primary antibodies: rabbit monoclonal p-MAPK antibody (Cell Signaling Technology, Beverly, MA, USA, 4370, 1:1000 diluted), rabbit monoclonal Bax antibody (Santa Cruz Biotechnology, Santa Cruz, CA, sc-7480, 1:1000), rabbit monoclonal Bcl-2 antibody (Santa Cruz Biotechnology, Santa Cruz, CA, sc-7382, 1:1000), rabbit monoclonal cleaved caspase 3 antibody (Santa Cruz Biotechnology, Santa Cruz, CA, sc-271028, 1:100), rabbit monoclonal LC3 antibody (Cell Signaling Technology, Beverly, MA, USA, 2775, 1:1000), rabbit polyclonal atg12 antibody (Santa Cruz Biotechnology, Santa Cruz, CA, sc-271688, 1:100) and mouse α-tubulin antibody (Cell Signaling Technology, Beverly, MA, USA, 3783S, 1:1000). After three washes with TBST, the membrane was incubated for 1 h with the secondary peroxidase-conjugated goat anti-mouse or anti-rabbit IgG antibodies (Zhongshan Golden Bridge, Beijing, China, ZDR-5307 or ZDR-5306, 1:1000) in TBST/5% BSA. The protein bands were visualized using a SuperSignal West Femto Maximum Sensitivity Substrate (Thermo Fisher Scientific, Rockford, IL, USA). The relative signal intensity was measured by ImageJ software.

2.7. Real-time quantitative PCR (RT-qPCR) analysis

Total RNA was isolated from oocytes using a TRNpure Total RNA Extraction Kit (Nobelab , Beijing , China) according to the manufacturer's instructions. The RNA content in each sample (150 mouse oocytes) was quantified by a NanoDrop 2000 nucleic acid quantifier (A260/280 nm). PrimeScript RT Reagent Kit (TaKaRa, Dalian, China) was used to reverse transcribe mRNA into cDNA. Each group of reverse transcription products, analysed in triplicate, was mixed with FastStart Universal SYBR Green Master (Roche, Switzerland) to evaluate the expression of the target gene. The PCR product was detected and analysed by CFX Manager (Bio-Rad, America). The primers are given in Table S1. The $2^{-\Delta\Delta CT}$ method was used to calculate the gene expression level using GAPDH as a reference gene.

2.8. Mechanical measurement

A pair of three-degrees-of-freedom micromanipulators was used to control the micropipette with a travel distance of 50 mm and a position resolution of 1 μm along each axis. A camera was connected to the microscope for visual detection, and the image was collected at 20 frames/s. Independently developed pneumatic syringes were connected to the micropipettes to provide negative pressure. A motorized XY stage was used to position the cell samples, which were placed in a 35 mm Petri dish.

The mechanical properties of the oocytes were characterized by measuring the hardness of the zona pellucida (ZP). Young's modulus was used to represent the ZP hardness. Here, we used the current general shell model (Khalilian et al., 2010) to estimate the Young's modulus of the mouse ZP, as shown in Fig. 2b. Young's modulus of the ZP was estimated by the following equation:

$$E_Z = 2C(h^*)(1-v^2)\left(\frac{\Delta P}{\Delta L/R_P}\right)$$

where v, assuming incompressibility ($v = 0.5$), was evaluated; h^* represented the oocyte's dimensionless thickness, which was defined as the ratio of the ZP thickness (h) to the micropipette radius (R_p); and $C(h^*)$ was a function of h^* and could be estimated by the following equation.

$$C(h^*) = \begin{cases} \frac{a + cln(h^*) + eln^2(h^*) + gln^3(h^*) + iln^4(h^*)}{1 + bln(h^*) + dln^2(h^*) + fln^3(h^*) + hln^4(h^*) + jln^5(h^*)} & 0.1 \le h^* \le 50 \\ 0.64395655 & h^* \ge 50 \end{cases}$$

$a = 1.070275412$, $b = 0.592405186$, $c = -0.44373788$, $d = 0.126723221$, $e = 0.721290633$,

$f = 0.074985305$, $g = -0.14390482$, $h = 0.027220129$, $i = 0.040156098$, $j = 0.00132358$.

2.9. Statistical analysis

Data were analysed by ANOVA using GraphPad Prism software and expressed as the mean ± SEM. Values of $p < 0.05$ were considered statistically significant. The fluorescence intensity of each oocyte was analysed by ImageJ software.

3. Results

3.1. Characterization of BHPF

The structure of BHPF was analysed by FTIR (Fig. S1b). For BHPF, the adsorption peaks at 1284.71 cm^{-1} and 3463.40 cm^{-1} corresponding to C-O and O-H in the phenolic hydroxyl group, respectively. The vibration absorption peaked in the benzene ring at 1592.38 cm^{-1} and 1607.75 cm^{-1}. Based on dynamic light scattering (DLS), Figs. S1c and d shows the particle size distribution of M16 medium and BHPF in M16 medium. Quantitative analysis showed that the aggregation size of M16 medium was 95.95 ± 8.13 nm and that the aggregation size of BHPF in M16 medium was 402.1 ± 6.36 nm (Fig. S1e, Table S2). The zeta potential of BHPF in M16 medium (−29.93 ± 8.29 mV) was increased compared to that of control M16 medium (−22.01 ± 5.70 mV, Fig. S1f, Table S2). Then, we investigated the effects of BHPF on the maturation of mouse oocytes. Mouse oocyte collection and *in vitro* culturing to different stages of the time axis are shown in Fig. S1g.

3.2. The effect of BHPF exposure on mouse oocyte maturation in vitro

The oocytes were harvested from the ovaries and cultured for 14 h *in vitro* with different concentrations (0, 50, 100, 200 and 400 μM) of BHPF. Our results showed that BHPF exposure exerted toxic effects on oocyte maturation and that the effect of BHPF was concentration dependent (Fig. 1a). As the concentration of BHPF increased, the polar body extrusion (PBE) rate of the mouse oocytes also decreased significantly (Fig. 1b). We found that 200 μM BHPF treatment increased cytoplasmic abnormalities in mouse oocytes. Cytoplasmic shrinkage and the cytoplasmic granulation of oocytes were observed after treatment with high concentrations of BHPF (400 μM).

We next examined the spindle assembly and chromosome alignment in mouse oocytes after BHPF exposure. Control oocytes at MII had a typical barrel-shaped spindle structure and arranged chromosomes (Fig. 1c). Conversely, BHPF exposure caused the spindle to exhibit an irregular microtubule distribution and a defective chromosome alignment in mouse oocytes *in vitro* (Fig. 1c). The proportion of abnormal spindles in the treatment group was significantly higher than that in the control group (Fig. 1d and e). The chromosome alignment was also

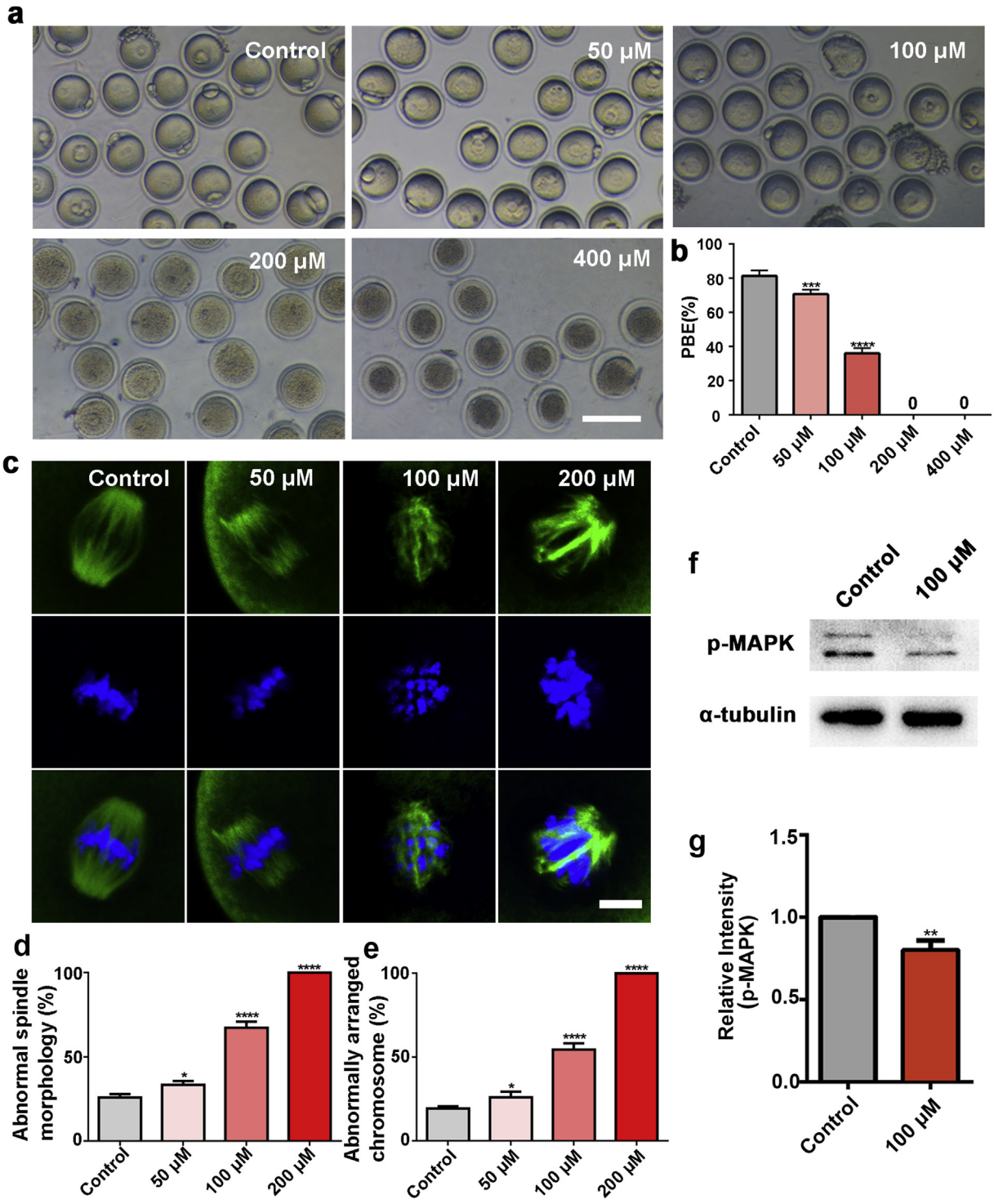

Fig. 1. Effects of BHPF on oocyte maturation *in vitro*. (a) The morphology of MII oocytes after 14 h of culture in the control and BHPF-treated groups. GV stage oocytes were harvested and cultured for 14 h. Bar: 100 μm. (b) Polar body extrusion (PBE) rates of mouse oocytes treated with 50, 100, 200 and 400 μM BHPF. (c) BHPF exposure caused spindle and chromosomal abnormalities in mouse oocytes. Oocytes were stained with α-tubulin antibody (green) and double-labelled with DAPI (blue). Bar: 10 μm. (d, e) Proportion of abnormal spindle and chromosome from the control and BHPF-treated groups. (f, g) The Western blot results showed that the expression of p-MAPK was significantly decreased after BHPF exposure. Data are shown as the means ± standard errors. *$p < 0.05$, **$p < 0.01$, ***$p < 0.001$, ****$p < 0.0001$. (For interpretation of the references to colour in this figure legend, the reader is referred to the Web version of this article.)

examined. For subsequent experiments, we chose 100 μM BHPF as the treatment concentration. To confirm spindle assembly disruption, p-MAPK, an important protein of microtubule organizing centres (MTOCs), was analysed in our study. After 100 μM BHPF exposure, the protein expression level of p-MAPK was significantly reduced (Fig. 1f and g).

3.3. BHPF exposure induced mechanical property changes in mouse oocytes

In this experiment, the average Rp value for all micropipettes employed was 11.2 ± 1.3 μm, and the average h value was 7.3 ± 0.9 μm. Fig. 2b shows the cell morphology at different BHPF concentrations. The cells showed obvious cytoplasmic shrinkage and cytoplasmic

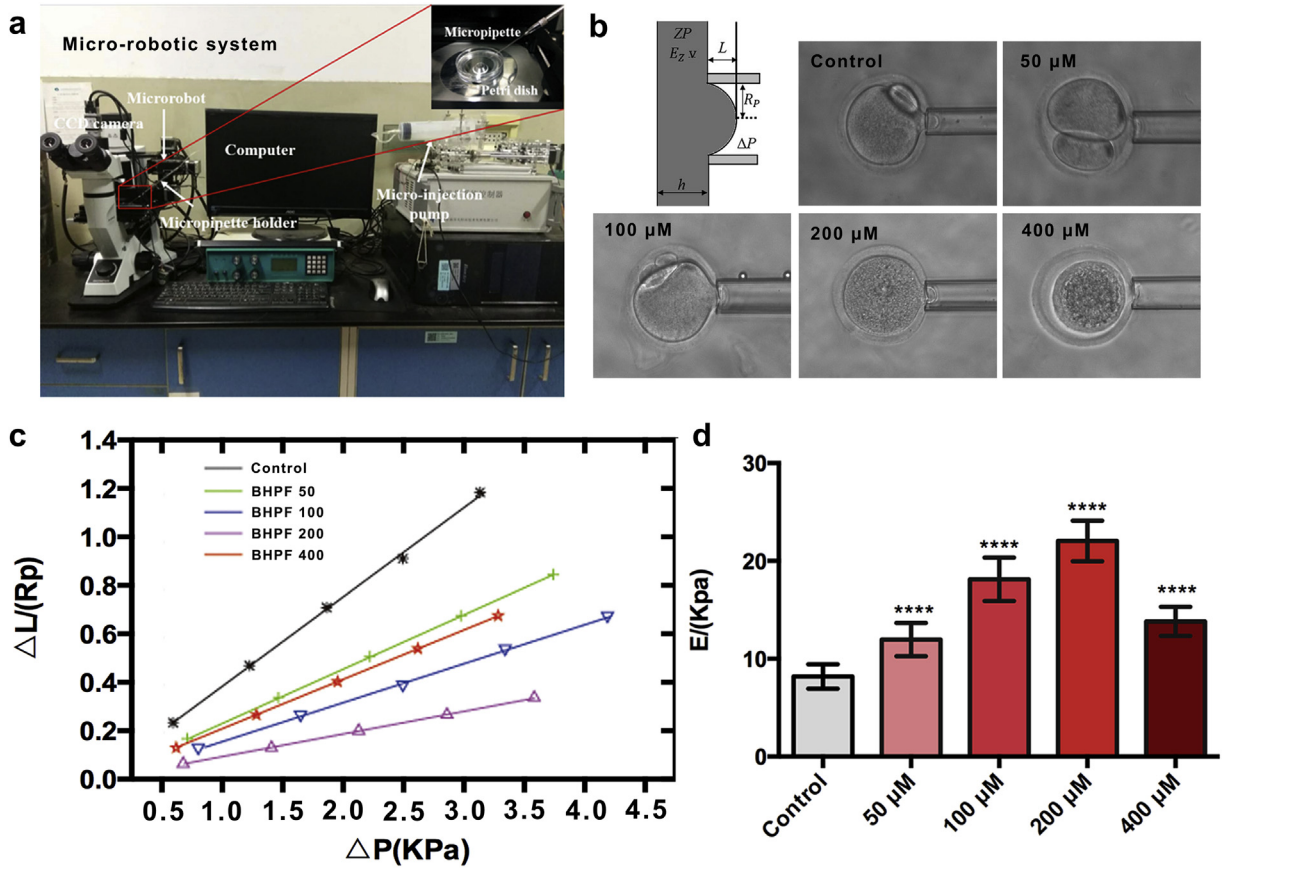

Fig. 2. Mechanical parameters were measured by a micromanipulation system. (a) The micromanipulation system for measuring the Young's modulus of the ZP. (b) The shell model to estimate the Young's modulus of the ZP and the cell morphology at different BHPF concentrations. (c) The relationship between the pressure and elongation of the ZP. (d) The Young's modulus of the ZP at different BHPF concentrations (50 μM, 100 μM, 200 μM and 400 μM). ****$p < 0.0001$.

granulation at a BHPF concentration of 400 μM. A pressure sensor was used to record the pressure. The relationship between pressure and ZP elongation is shown in Fig. 2c. Five groups of pressure-length data from each mouse oocyte were used for linear regression to obtain Young's modulus. The reported Young's modulus of the ZP, which was measured by various experimental techniques, ranged from 8.26 to 17.9 kPa (Murayama et al., 2008; Sun et al., 2003). Using the micropipette aspiration technique, the Young's modulus of the control group was 8.2 ± 1.2 kPa. The Young's modulus of the ZP changed after BHPF treatment. The Young's modulus of the ZP gradually increased when the concentration of BHPF increased from 50 μM to 200 μM. The Young's modulus of the ZP was significantly reduced by BHPF at a concentration of 400 μM, as shown in Fig. 2d. The results demonstrate that BHPF could cause ZP hardening. Excessive concentrations of BHPF cause oocyte cytoplasmic shrinkage and cytoplasmic granulation.

3.4. BHPF exposure induced oxidative stress, resulting in DNA double-strand breakage, and interfered with mitochondrial function in mouse oocytes

We next investigated whether BHPF could cause oxidative stress in mouse oocytes. The concentration of BHPF (0, 50, 100, and 200 μM) was consistent with the previous set of experiments. As shown in Fig. 3a, the ROS fluorescence intensity in BHPF-treated oocytes (100 and 200 μM) was significantly higher than that in control group oocytes. However, there was no significant difference in the degrees of oxidative stress in the low concentration (50 μM) and the control groups. Furthermore, the increase in the oxidative stress level in oocytes has a concentration dependence on BHPF. Quantitative analysis showed that the relative fluorescence intensity increased as the BHPF concentration increased, which was consistent with the staining results (Fig. 3b and c).

Since reactive oxygen species are associated with DNA damage, we next explored whether exposure to BHPF damaged mouse oocyte DNA. As shown in Fig. 3d, γ-H2AX was stained as a marker to label DNA double-strand breaks (DSBs) in oocytes. The γ-H2AX in the BHPF-treated groups had brighter foci than that in the control group, which implied the generation of DNA damage (Fig. 3d). Quantitative analysis showed that the relative fluorescence intensity of γ-H2AX increased as the BHPF concentration increased, which was consistent with the staining results (Fig. 3e). Furthermore, mitochondrial function is associated with ROS production, which can be used as an important indicator of oocyte quality. We next explored whether BHPF exposure adversely affects oocyte mitochondrial function. We used JC-1 to evaluate the mitochondrial membrane potential, and the control oocytes exhibited a high mitochondrial membrane potential, showing strong red and weak green JC-1 fluorescence (Fig. 3f). Compared with that of the control group, BHPF treatment decreased the mitochondrial membrane potential, showing weak red and strong green JC-1 fluorescence in oocytes (Fig. 3f). Quantitative analysis showed that the ratio of red to green JC-1 fluorescence decreased significantly after BHPF exposure, which was consistent with the staining results (Fig. 3g).

3.5. BHPF in vitro exposure induced early apoptosis and autophagy in mouse oocytes

We next assessed the levels of autophagy and apoptosis in oocytes after BHPF exposure. As shown in Fig. 4a, annexin-V was stained as an early apoptotic signal marker, and early apoptotic signals arose in BHPF oocytes. Quantitative analysis indicated that apoptotic oocytes were

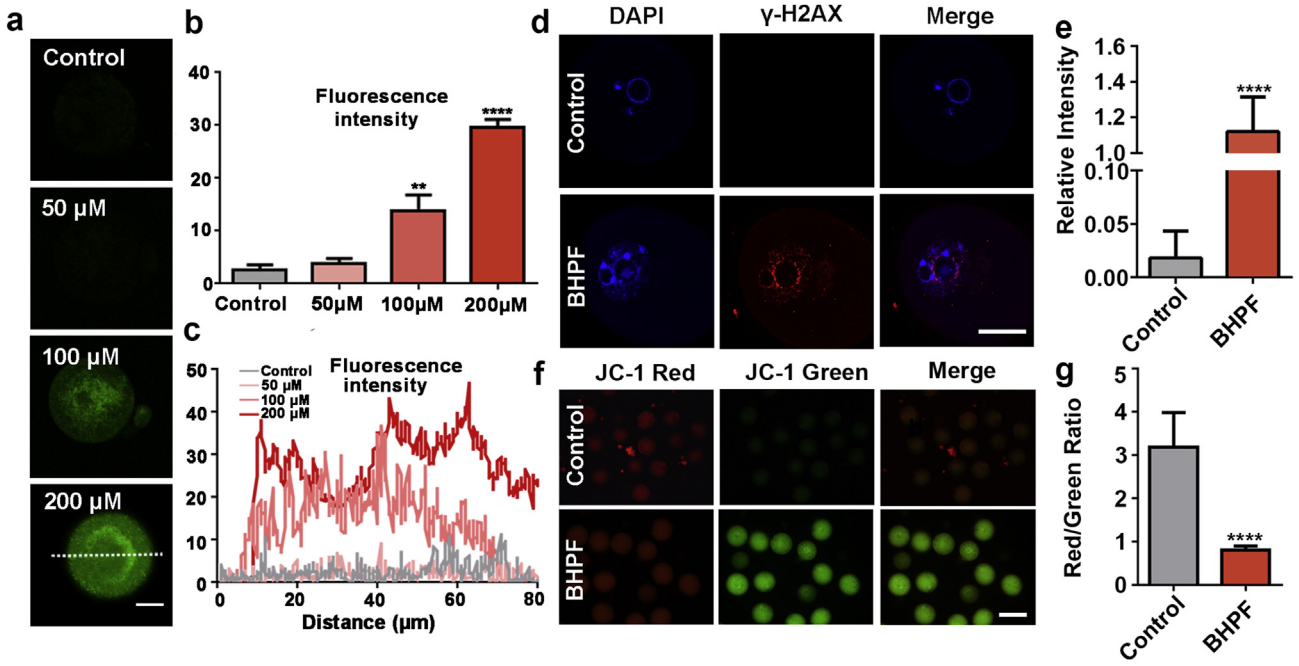

Fig. 3. BHPF exposure caused oxidative stress, DNA damage and mitochondrial membrane potential reduction in mouse oocytes. (a) Fluorescently stained images of oocytes in the control group and BHPF exposure groups at concentrations of 50, 100, and 200 μM. Scale bar indicates 25 μm. (b, c) Fluorescence intensity quantification of the oxidative stress level (n = 50). (d) Fluorescently stained images of oocytes in the control group and BHPF exposure groups at 100 μM. DNA: blue. γ-H2AX: red. Scale bar indicates 25 μm. (e) Fluorescence intensity quantification of the DNA damage level (n = 50). (f) Fluorescenly stained images of oocytes in the control and 100 μM BHPF exposure groups. Scale bar indicates 100 μm. (g) Ratio of red to green JC-1 fluorescence intensity quantifying the mitochondrial membrane potential (n = 50). **p < 0.01, ****p < 0.0001. (For interpretation of the references to colour in this figure legend, the reader is referred to the Web version of this article.)

significantly increased after 14 h of BHPF exposure, which was consistent with the staining results (Fig. 4b). We also assessed the LC3 levels in oocytes by immunofluorescence staining (Fig. 4d), which showed that the LC3 fluorescence levels were increased after 14 h of BHPF exposure (Fig. 4e). The Western blot analyses showed that the Bax, cleaved caspase-3, LC3 and Atg12 protein levels were significantly increased in the BHPF treatment group; however the Bcl-2 protein levels were decreased after BHPF exposure (Fig. 4g–j). qRT-PCR analyses showed that the Bax, caspase-3, LC3, Atg14, and Beclin mRNA expression levels and the Bcl-xl and mTOR expression levels were changed in the BHPF-treated oocytes (Fig. 4c, f). The increased expression levels of Bax and Atg14 were significantly different. Thus, BHPF exposure induced early apoptosis and autophagy in the mouse oocyte.

3.6. BHPF exposure affected ovarian and follicle development

To further explore the effects of BHPF on the development of mouse oocytes, we conducted *in vivo* experiments to investigate the effects on ovarian and follicle development. As shown in Fig. 5, the ovarian morphology and ratio of ovarian weight to body weight were not significantly different between the control and BHPF-treated groups (Fig. 5a, c). Quantitative analysis showed that the percentage of atretic follicles significantly increased as the BHPF concentration increased (Fig. 5b, d). After BHPF exposure, the Bax and cleaved caspase-3 protein levels were significantly increased, as determined by Western blot; however, the Bcl-2 protein levels were decreased (Fig. 5f). qRT-PCR analyses showed that the CAT, GPX3 and SOD2 mRNA expression levels were significantly increased in BHPF-treated oocytes compared to that in control oocytes (Fig. 5g), indicating that exposure to BHPF *in vivo* promotes apoptosis and oxidative stress in ovarian tissue (Sun et al., 2012).

3.7. BHPF exposure induced significant oxidative stress and had no effect on spindle assembly in mouse oocytes in vivo

We next investigated whether BHPF could induce oxidative stress in mouse oocytes *in vivo*. As shown in Fig. 6a, the ROS fluorescence intensity in BHPF-treated oocytes was significantly higher than that in control group oocytes. Furthermore, the increase in the oxidative stress level of oocytes had a concentration dependence on BHPF. Quantitative analysis results were consistent with the staining results (Fig. 6c). However, the oocytes had a typical barrel-shaped spindle structure and arranged chromosomes at the equator of the spindle after BHPF exposure *in vivo* (Fig. 6b). The proportion of abnormal spindles in the treatment group was not significantly different from that in the control group (Fig. 6d).

4. Discussion

Due to their adverse effects on human health, endocrine disruptors chemicals have received widespread attention. BHPF is considered to be a substitute for BPA and may impair female the reproductive capacity of female mice. However, there are few studies on the toxicity of BHPF on oocyte development and maturation. In this study, we hypothesized that exposure to BHPF causes oocyte polar body extrusion failure in *in vitro* maturation and inhibits cell cycle progression and oocyte maturation. Then, we explored the toxicity of BHPF and its underlying mechanisms in the following areas: oxidative stress, spindle assembly, DNA damage, mitochondrial membrane potential, autophagy, apoptosis, and ovarian damage (Fig. 7).

To confirm our hypothesis, we first cultured oocytes *in vitro* for 14 h and found that the rate of oocyte polar bodies was decreased in the BHPF treatment group (Fig. 1). Cytoplasmic shrinkage and cytoplasmic granulation of oocytes were observed in the high-concentration BHPF treatment group (400 μM). This result suggests that BHPF has a negative influence on oocyte maturation. Next, we examined the spindle

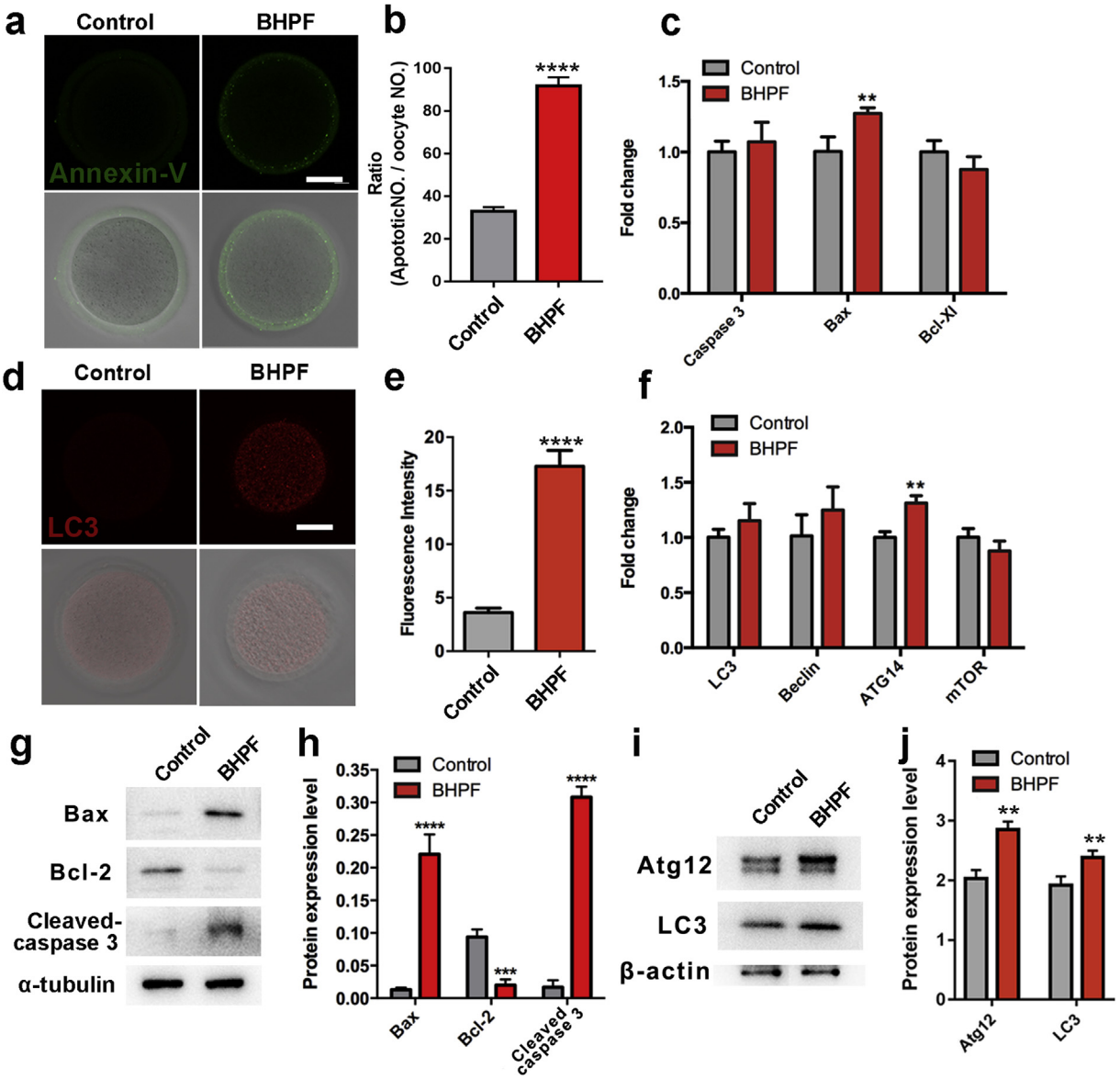

Fig. 4. BHPF exposure induced early apoptosis and autophagy in mouse oocytes *in vitro*. (a) Fluorescently stained images of oocytes in the control and 100 μM BHPF 14 h exposure groups. Annexin-V: green. Scale bar indicates 10 μm. (b) Percentages of oocytes exhibiting early-stage apoptosis. (c) Relative mRNA expression of three genes related to apoptosis in the control and BHPF exposure groups. (d) Immunofluorescence staining of LC3 in oocytes after 14 h of BHPF treatment. LC3: red. Bar: 25 μm. (e) The fluorescence intensity quantification of LC3 expression (n = 50). (f) The mRNA expression of LC3, Beclin, Atg14 and mTOR in mouse oocytes. (g, h) Western blot showed the expression of apoptosis-related proteins and autophagy-related proteins in the control and BHPF-treated groups. (h, j) Relative intensity of apoptosis-related protein expression and autophagy-related protein expression in mouse oocytes. **p < 0.01, ***p < 0.001, ****p < 0.0001. (For interpretation of the references to colour in this figure legend, the reader is referred to the Web version of this article.)

morphology and chromosome arrangement of BHPF-exposed oocytes to study the factors underlying the decreased maturation rate of oocytes. Our findings showed that most BHPF-treated oocytes had abnormal meiosis spindle morphology and chromosome alignment. The MII oocytes were exposed to toxic environmental components to not only disrupt the symmetrical barrel structure but also to disrupt the equatorial chromosome for chromatid segregation (Khan et al., 2016). In addition, excessive ROS production may be the cause of meiosis defects in mouse oocytes (Han et al., 2017). The p-MAPK protein level in the BHPF group was dramatically decreased compared with that in the control group. p-MAPK is a microtubule-related protein involved in cell differentiation and apoptosis and is necessary for stabilizing spindle assembly in mouse oocytes (Zhang et al., 2016; Zhu et al., 2016). MTOC dysfunction, caused by the abnormal expression of p-MAPK, is an important factor leading to defective spindle assembly in BHPF-treated oocytes. Our results showed that BHPF exposure-induced MTOC dysfunction is the main factor underlying subsequent spindle defects.

It is also important to understand the physiological and pathological processes of oocytes based on their mechanical properties. Our previous studies have shown that the quality of oocytes affects the mechanical properties of the zona pellucida (Jia et al., 2018). The mechanical properties of oocytes are usually characterized by measuring the hardness of the zona pellucida. In this study, the hardness of the oocyte zona pellucida increased as the BHPF concentration increased (0–200 μM). This phenomenon may have occurred because the number of cross-linked protein (ZP1 between ZP2 and ZP3) units increased, causing the zona pellucida to harden (Sun et al., 2005). However, when the BHPF treatment concentration reached 400 μM, the hardness of the oocyte zona pellucida was significantly decreased but remained higher than that of the control group. We speculate that the cytoplasmic

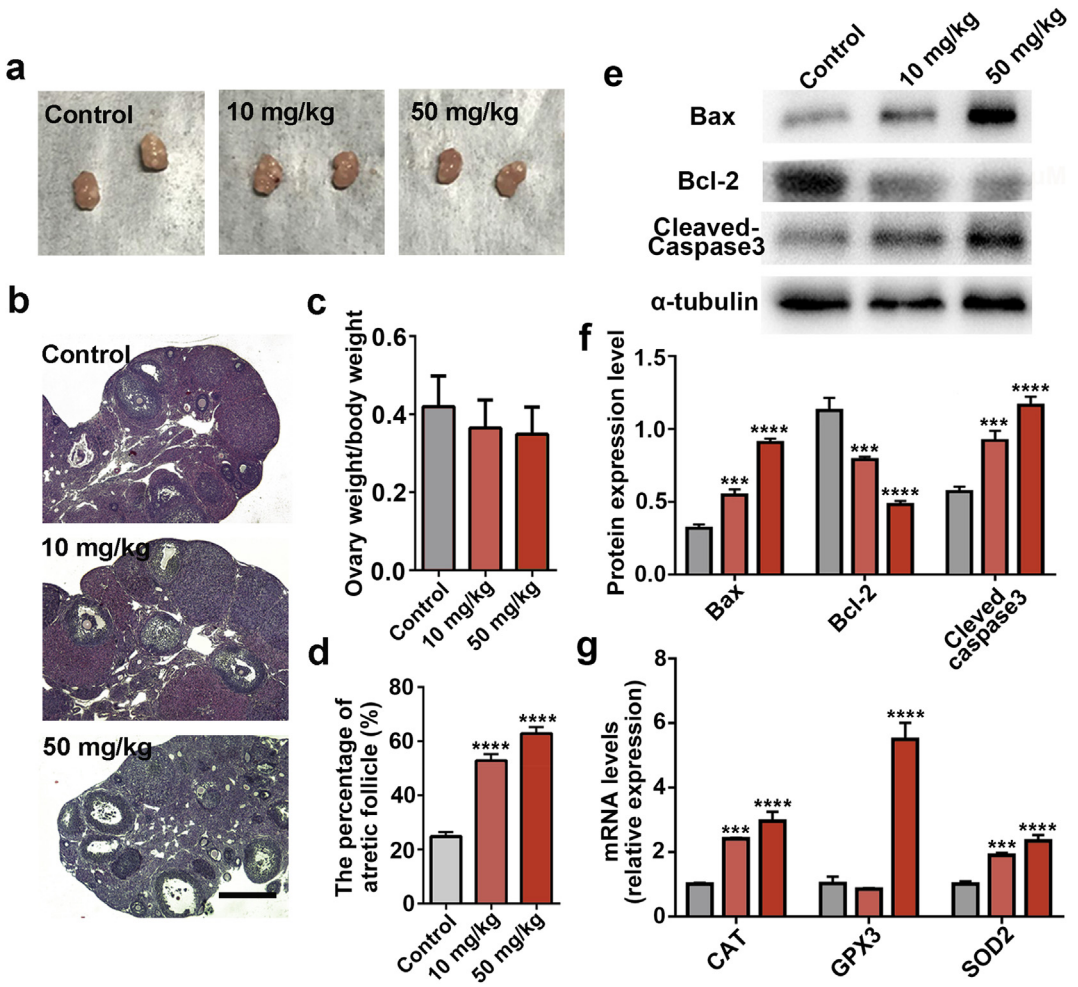

Fig. 5. Effect on ovarian and follicle development after BHPF exposure in mice. (a) Images of ovarian morphology in control mice and in 2, 10, and 50 mg/kg BHPF-treated mice. (b) Histological sections of ovaries from the control and BHPF exposure groups at different concentrations that were stained with haematoxylin and eosin. Scale bar indicates 100 μm. (c, d) Quantitative analysis of follicles at different stages in ovarian sections based on the ratio of ovary weight to body weight and the percentage of atretic follicles. (e, f) Western blot showing that Bax and Cleaved caspase 3 protein levels were increased, while the Bcl-2 protein levels were decreased after BHPF exposure. (g) The expression of oxidative stress-related genes in mouse ovaries. Data are shown as the means ± standard errors. ***$p < 0.001$, ****$p < 0.0001$.

shrinkage of oocytes may be one factor underlying the decreased hardness of the zona pellucida.

ROS are produced by oocyte metabolism or the oocyte environment (Sugino, 2005), which is responsible for the poor quality of oocytes (Tamura et al., 2010). In this study, increase ROS levels were observed in the BHPF group compared with those in the control group. The level of oxidative stress increased rapidly as the BHPF concentration increased. Mitochondria are the main place of producing the ROS and the most sensitive part of ROS (Chen et al., 2003). A previous study demonstrated that the accumulation of ROS leads to cells being in a redox state, which plays a role in apoptosis induction (Lord and Aitken, 2013; Tatemoto et al., 2000; Zhang et al., 2006). Mammalian oocytes and embryos are exceptionally sensitive to ROS (Van, 2011). Our findings indicate that BHPF exposure induces excess ROS in mouse oocytes, indicating oxidative stress, which is the reason underlying the failure of oocyte maturation (Yue et al., 2016). In addition, bisphenol AF (BPAF), a fluorinated homolog of BPA, can be used as an endocrine disruptor by acting as an oestrogen receptor agonist or antagonist (Ding et al., 2017). BPAF exposure may negatively impact female fertility by influencing cytoskeleton kinetics, inducing oxidative stress, increasing DNA damage and altering epigenetic modifications. Bisphenol S (BPS), another alternative to BPA, has been shown to have negative effects on the cell maturation of porcine oocytes (Žalmanová et al., 2017), especially during the meiotic cell cycle, tubulin fibre formation, maternal mRNA generation and cumulus cell expansion. Recent evidence has suggested that BPS is capable of inducing changes in embryonic neural and endocrine systems (Kinch et al., 2015).

ROS, which are produced as a result of endogenous metabolism and/or exposure to environmental poisons, constitute an important type of DNA damage agent (Yang et al., 2011). In addition to destroying DNA directly, ROS may also damage DNA indirectly by reacting to lipids, proteins, and other cellular components (Irina et al., 2009; Marnett, 1999; Yang et al., 2011). Our results showed that the fluorescence intensity of γ-H2AX in BHPF-treated oocytes was higher than that in the control oocytes. The histone H2A variant H2AX is phosphorylated at serine residue 139 (Fei et al., 2014; Rogakou et al., 1998) after DNA damage. Because phosphorylation products can accumulate at sites of DNA damage, they are used as a marker of DNA damage (Fei et al., 2014). We speculate that increased DNA damage may be mediated by BHPF-induced ROS generation (Halliwell, 1999). Moreover, recent studies have confirmed that DNA damage induced meiosis stagnation and apoptosis in mouse oocytes (Collins et al., 2015; Fei et al., 2014; Shi et al., 2018). Mitochondria are the main energy-producing organelles in oocytes, and their activity is closely related to the quality of oocytes (Chen et al., 2003; Ou et al., 2012). The mitochondria of oocytes were exposed to JC1 to determine the mitochondrial

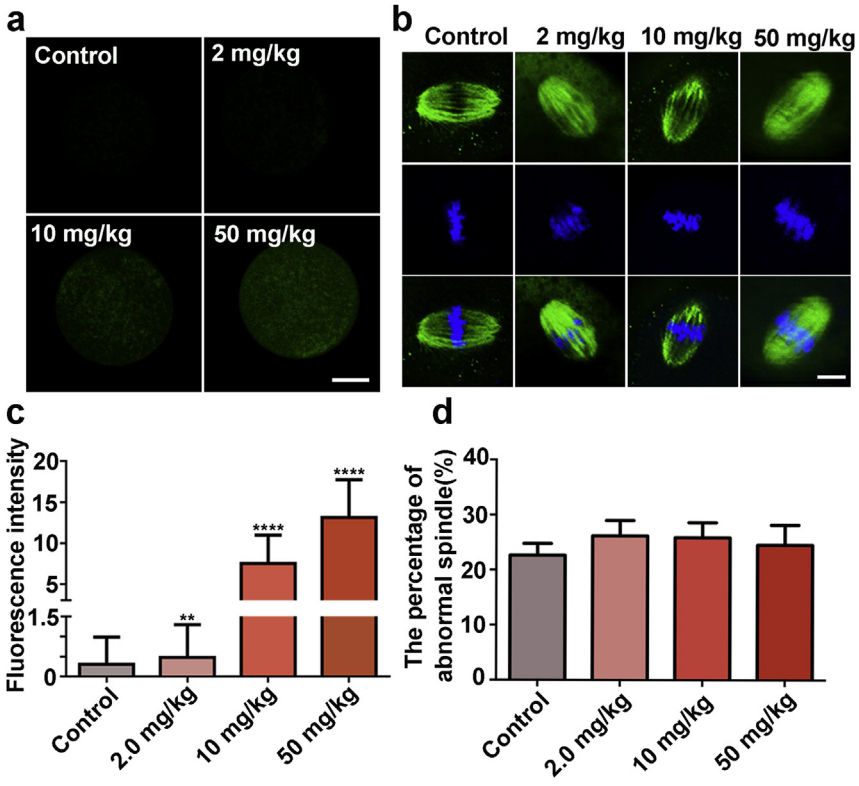

Fig. 6. BHPF exposure induced oxidative stress and had no effect on spindle assembly in mouse oocytes. (a) Fluorescently stained images of oocytes in the control group and the 2, 10, and 50 mg/kg BHPF exposure groups. Scale bar: 25 μm. (b) Images of spindle morphology in the control and BHPF-treated groups. (c) Fluorescence intensity quantification of the oxidative stress level (n = 50). (d) Proportion of abnormal spindles in the control and BHPF-treated groups. **p < 0.01, ****p < 0.0001.

membrane potential; the dye emits a red fluorescence in active mitochondria and a green fluorescence in inactive mitochondria. The results showed that the red and green fluorescence ratios in the exposed group were significantly decreased, and the low values indicated that the mitochondrial activity was decreased. The electron transfer chain in the mitochondrial endometrium participates in the generation of energy (Gurung et al., 2015). With rupture of the electron transfer chain, ROS are constantly produced to create cytotoxicity (Gurung et al., 2015). Hence, we can infer that the increase in ROS in BHPF-exposed oocytes is a major factor underlying the decreased mitochondrial

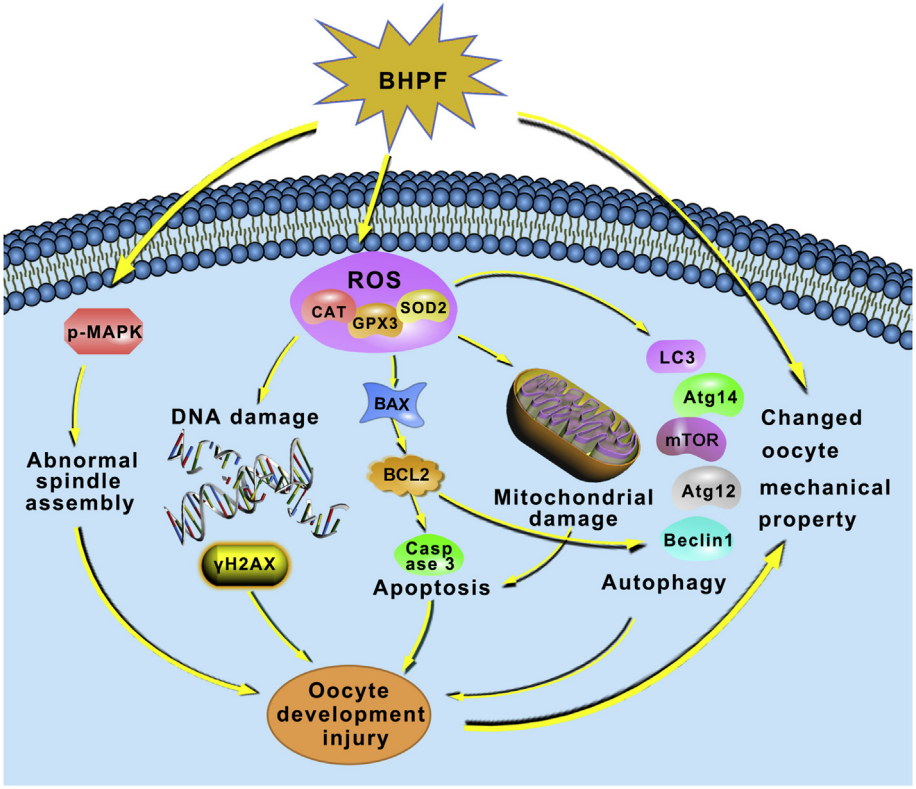

Fig. 7. Potential mechanism of BHPF-induced cytotoxicity on mouse oocytes.

activity.

Apoptosis in oocytes might be involved in the mechanism by which oxidative stress mediates damage (Chaube et al., 2015). Thus, we explored early apoptosis in mouse oocytes treated with BHPF. Increasing evidence indicates that oocytes exposed to endocrine disruptors can induce early apoptosis due to elevated levels of oxidative stress (Guo et al., 2017; Wang et al., 2016). The protein levels of apoptosis-related factors (Bax and Bcl-2) confirmed the effect of BHPF on the apoptosis of oocytes. The mRNA expression of Bax and Bcl-xl also verified that apoptosis occurred in BHPF-treated oocytes. Previous studies have shown that ROS promote autophagy activation and that the occurrence of autophagy can reduce oxidative damage (Scherzshouval and Elazar, 2011). The increased expression levels of LC3 and Atg 14 and the mRNA expression of autophagy-related genes validated the hypothesis that BHPF induces oocyte autophagy. Increased autophagy levels may be one of the reasons underlying the failure of oocytes to mature *in vitro*.

The ovaries can produce reactive oxygen species in the stages of follicle development and ovulation due to active metabolism (Chaube et al., 2015). Excessive production of ROS in the ovary will cause oxidative stress, which may affect the oocyte quality and assisted reproductive technology (ART) outcome. Studies have shown that when cells are compromised by a harmful environment, increase expression of the associated antioxidant genes CAT, SOD2 and GPX3 can reduce hydrogen peroxide and organic peroxides, protecting cells from oxidative damage (Jian et al., 2008; Wang et al., 2018). The increased CAT, GPX3 and SOD2 expression levels in the BHPF-treated group herein indicated that BHPF induces oxidative stress in the ovary and might further inhibit oocyte maturation and development. A recent study showed that clomiphene citrate, an antioestrogenic drug, induces ROS-mediated apoptosis in granulosa cells and oocytes to accelerate the deterioration of oocyte quality (Chaube et al., 2015). Therefore, we hypothesized that BHPF, which has antioestrogenic activity, induces apoptosis by increasing ROS levels, thereby affecting oocyte maturation. Our study found that BHPF *in vivo* exposure had no significant effect on the ovarian/weight ratio in mice. However, quantitative protein analysis indicated that *in vivo* exposure to BHPF increased the apoptosis level in the ovary, especially in the high concentration group (50 mg/kg). This phenomenon specifically manifested as increased Bax expression and downregulated Bcl-2 expression, suggesting that the *in vivo* exposure to BHPF induced ovarian damage. Studies have shown that Bcl-2 proteins play a key role in inhibiting apoptosis (Yang and Rajamahendran, 2002), which could explain why the protein expression of Bcl-2 was decreased in BHPF-exposed oocytes in our study. Our study found that the proportion of atresia follicles was increased after BHPF exposure, which might be related to the increased levels of ovarian cell apoptosis (Cui et al., 2011). These results suggest that BHPF increases the percentage of atretic follicles, possibly by modulating the elements in the apoptosis signaling pathway (Moon et al., 2009; Zhu et al., 2018).

In conclusion, we investigated the toxic effects of BHPF on the maturation of mouse oocytes and the possible mechanisms in this study. Our results show that the exposure of oocytes to BHPF reduces the expression of p-MAPK and destroys the spindle morphology, thus affecting the maturation of oocytes. After BHPF treatment, the level of ROS in the oocytes increased, which induced oxidative stress. In addition, with the occurrence of oxidative stress, the mitochondrial function and DNA of oocytes were impaired to a certain extent, inducing apoptosis and autophagy. The exposure of mouse oocytes to BHPF has a negative impact on oxidative stress, meiosis spindle morphology, DNA damage, mitochondrial function, apoptosis, autophagy, and ovarian development. Our research provides a potential mechanism for BHPF toxicity in oocytes.

Author contributions

X. Z. F. and Z. Z. J. conceived and designed the experiments. Z. Z. J., H. Y. W., S. Z. Z., Z. Y. F., L. N. W. and J. W. Z. performed the experiments. Z. Z. J., H. Y. W., S. Z. Z. and Z. Y. F. made an important contribution to data analysis and wrote the manuscript. X. Z. F., D. F. F. and X. Z. made important contributions to the discussion and reviewed the manuscript. All authors discussed the results and implications and reviewed the manuscript at all stages.

Funding sources

This work was supported by the Special Fund for Basic Research on Scientific Instruments of the Chinese National Natural Science Foundation [grant nos: 61327802, 61127006], and the National Basic Research Program (973 program) of China [grant no: 2015CB856500].

Acknowledgment

This project was initiated in the State Key Laboratory of Medicinal Chemical Biology at Nankai University. The authors declare that there are no conflicts of interest.

Appendix A. Supplementary data

Supplementary data to this article can be found online at https://doi.org/10.1016/j.ecoenv.2019.05.019.

References

Cabaton, N.J., et al., 2011. Perinatal exposure to environmentally relevant levels of bisphenol A decreases fertility and fecundity in CD-1 mice. Environ. Health Perspect. 119, 547–552.
Chaube, S.K., et al., 2015. Clomiphene citrate induces ROS-mediated apoptosis in mammalian oocytes. Open J. Apoptosis 3, 52–58.
Chen, Q., et al., 2003. Production of reactive oxygen species by mitochondria: Central role of complex III. J. Biol. Chem. 278, 36027.
Collins, J.K., et al., 2015. DNA damage induces a meiotic arrest in mouse oocytes mediated by the spindle assembly checkpoint. Nat. Commun. 6, 8553.
Council N, 2011. Guidance for the Description of Animal Research in Scientific Publications. National Academies Press (3).
Cui, L.L., et al., 2011. Tumor necrosis factor α knockout increases fertility of mice. Theriogenology 75, 867–876.
Dai, Z., et al., 2009. Kinetics and thermal properties of epoxy resins based on bisphenol fluorene structure. Eur. Polym. J. 45, 1941–1948.
Ding, Z.M., et al., 2017. Bisphenol AF negatively affects oocyte maturation of mouse *in vitro* through increasing oxidative stress and DNA damage. Chem. Biol. Interact. 278, 222–229.
Fei, L., et al., 2014. Different fates of oocytes with DNA double-strand breaks *in vitro* and *in vivo*. Cell Cycle 13, 2674–2680.
Geens, T., et al., 2012. A review of dietary and non-dietary exposure to bisphenol-A. Food Chem. Toxicol. 50, 3725–3740.
Guo, J., et al., 2017. The possible molecular mechanisms of bisphenol A action on porcine early embryonic development. Sci. Rep. 7, 8632.
Gurung, P., et al., 2015. Mitochondria: Diversity in the regulation of the NLRP3 inflammasome. Trends Mol. Med. 21, 193–201.
Halliwell, B., 1999. Oxygen and nitrogen are pro-carcinogens. Damage to DNA by reactive oxygen, chlorine and nitrogen species: Measurement, mechanism and the effects of nutrition. Mutat. Res. Genet. Toxicol. Environ. Mutagen 443, 37–52.
Han, L., et al., 2017. Melatonin protects against maternal obesity-associated oxidative stress and meiotic defects in oocytes via the SIRT3-SOD2-dependent pathway. J. Pineal Res. 63, 12431–12443.
Irina, G.M., et al., 2009. Chemistry and biology of DNA containing 1,N2-deoxyguanosine adducts of the α,β-unsaturated aldehydes acrolein, crotonaldehyde, and 4-hydroxynonenal. Chem. Res. Toxicol. 22, 759.
Jia, Z., et al., 2018. Resveratrol reverses the adverse effects of a diet-induced obese murine model on oocyte quality and zona pellucida softening. Food Function 9, 2623–2633.
Jian, D., et al., 2008. Nrf2-Mediated transcriptional induction of antioxidant response in mouse embryos exposed to ethanol *in vivo*: Implications for the prevention of fetal alcohol spectrum disorders. Antioxidants Redox Signal. 10, 2023–2033.
Jiao, X.-F., et al., 2019. Effects of acute fluorene-9-bisphenol exposure on mouse oocyte *in vitro* maturation and its possible mechanisms. Environ. Mol. Mutagen. 60, 243–253.
Khalilian, M., et al., 2010. Estimating Young's modulus of zona pellucida by micropipette aspiration in combination with theoretical models of ovum. J. R. Soc. Interface 7, 687–694.

Khan, S.N., et al., 2016. Peroxynitrite deteriorates oocyte quality through disassembly of microtubule organizing centers. Free Radical Biol. Med. 91, 275–280.
Kinch, C.D., et al., 2015. Low-dose exposure to bisphenol A and replacement bisphenol S induces precocious hypothalamic neurogenesis in embryonic zebrafish. Proc. Natl. Acad. Sci. U. S. A. 112, 1475–1480.
Korshak, V.V., et al., 1971. Synthesis of epoxy polymers from bisphenols with bulky substituents ☆. Polym. Sci. 13, 170–176.
Liu, W., et al., 2008. Synthesis and characterisation of 9,9-bis(4-hydroxyphenyl)-fluorene catalysed by cation exchanger. Pigment Resin Technol. 37, 9–15.
Liu, Y., et al., 2015. Activation of α7 nicotinic acetylcholine receptors protects astrocytes against oxidative stress-induced apoptosis: Implications for Parkinson's disease. Neuropharmacology 91, 87–96.
Lord, T., Aitken, R.J., 2013. Oxidative stress and ageing of the post-ovulatory oocyte. Reproduction 146, R217–R227.
Marnett, L.J., 1999. Lipid peroxidation—DNA damage by malondialdehyde. Mutat. Res. Fund Mol. Mech. Mutagen 424, 83–95.
Meng, X.Q., et al., 2016. Subcellular localization of proline-rich tyrosine kinase 2 during oocyte fertilization and early-embryo development in mice. J. Reprod. Dev. 62, 351–358.
Moon, H.J., et al., 2009. Lactational coumestrol exposure increases ovarian apoptosis in adult rats. Arch. Toxicol. 83, 601–608.
Murayama, Y., et al., 2008. Elasticity measurement of zona pellucida using a micro tactile sensor to evaluate embryo quality. J. Mammalian Ova Res. 25, 8–16.
Ou, X.H., et al., 2012. Maternal insulin resistance causes oxidative stress and mitochondrial dysfunction in mouse oocytes. Hum. Reprod. 27, 2130–2145.
Patisaul, H.B., Adewale, H.B., 2009. Long-term effects of environmental endocrine disruptors on reproductive physiology and behavior. Front. Behav. Neurosci. 3, 10.
Perkins, A.T., et al., 2016. Oxidative stress in oocytes during midprophase induces premature loss of cohesion and chromosome segregation errors. Proc. Natl. Acad. Sci. U. S. A. 113, E6823–E6830.
Rizos, D., et al., 2002. Consequences of bovine oocyte maturation, fertilization or early embryo development *in vitro* versus *in vivo*: Implications for blastocyst yield and blastocyst quality. Mol. Reprod. Dev. 61, 234–248.
Rogakou, E.P., et al., 1998. DNA double-stranded breaks induce histone H2AX phosphorylation on serine 139. J. Biol. Chem. 273, 5858–5868.
Scherzshouval, R., Elazar, Z., 2011. Regulation of autophagy by ROS: Physiology and pathology. Trends Biochem. Sci. 36, 30–38.
Shi, F., et al., 2018. Melatonin reduces two-cell block via nonreceptor pathway in mice. J. Cell. Biochem. 119, 9380–9393.
Sugino, N., 2005. Reactive oxygen species in ovarian physiology. Reproductive Med. Biol. 4, 31–44.
Sun, Y., et al., 2012. 2,5-Hexanedione induces human ovarian granulosa cell apoptosis through BCL-2, BAX, and CASPASE-3 signaling pathways. Arch. Toxicol. 86, 205–215.
Sun, Y., et al., 2005. Investigating protein structure change in the zona pellucida with a microrobotic system. Int. J. Robot. Res. 24, 211–218.
Sun, Y., et al., 2003. Mechanical property characterization of mouse zona pellucida. IEEE Trans. NanoBioscience 2, 279.
Susiarjo, M., et al., 2015. Bisphenol A exposure disrupts metabolic health across multiple generations in the mouse. Endocrinology 156, 2049–2058.
Susiarjo, M., et al., 2017. Bile acids and tryptophan metabolism are novel pathways involved in metabolic abnormalities in BPA-exposed pregnant mice and male offspring. Endocrinology 158, 2533–2542.
Tamura, H., et al., 2010. Oxidative stress impairs oocyte quality and melatonin protects oocytes from free radical damage and improves fertilization rate. J. Pineal Res. 44, 280–287.
Tang, Y., et al., 2015. Icariin promotes angiogenic differentiation and prevents oxidative stress-induced autophagy in endothelial progenitor cells. Stem Cell. 33, 1863–1877.
Tatemoto, H., et al., 2000. Protection of porcine oocytes against apoptotic cell death caused by oxidative stress during *in vitro* maturation: Role of cumulus cells. Biol. Reprod. 63, 805–810.
Van, B.J., 2011. Mitochondrial function in the human oocyte and embryo and their role in developmental competence. Mitochondrion 11, 797–813.
Vandenberg, L.N., et al., 2009. Bisphenol-A and the great divide: A review of controversies in the field of endocrine disruption. Endocr. Rev. 30, 75.
Wang, C., et al., 2017. Low concentration of BPA induces mice spermatocytes apoptosis via GPR30. Oncotarget 8, 49005–49015.
Wang, T., et al., 2016. The toxic effects and possible mechanisms of Bisphenol A on oocyte maturation of porcine*in vitro*. Oncotarget 7, 32554–32565.
Wang, X., et al., 2018. Preliminary investigation on cytotoxicity of fluorinated polymer nanoparticles. J. Environ. Sci. 69, 217–226.
Wang, Y.Q., Zhang, H.M., 2015. Exploration of binding of bisphenol A and its analogues with calf thymus DNA by optical spectroscopic and molecular docking methods. J. Photochem. Photobiol. B Biol. 149, 9.
Xiao, S., et al., 2011. Preimplantation exposure to bisphenol A (BPA) affects embryo transport, preimplantation embryo development, and uterine receptivity in mice. Reprod. Toxicol. 32, 434–441.
Yang, M.Y., Rajamahendran, R., 2002. Expression of Bcl-2 and Bax proteins in relation to quality of bovine oocytes and embryos produced *in vitro*. Anim. Reprod. Sci. 70, 159–169.
Yang, Y., et al., 2011. Occurrence, biological consequences, and human health relevance of oxidative stress-induced DNA damage. Chem. Res. Toxicol. 29, 2008.
Yue, Z., et al., 2016. Exposure to HT-2 toxin causes oxidative stress induced apoptosis/autophagy in porcine oocytes. Sci. Rep. 6, 33904.
Žalmanová, T., et al., 2017. Bisphenol S negatively affects the meotic maturation of pig oocytes. Sci. Rep. 7, 485.
Zhang, J.H., et al., 2016. Mitofusin-2 is required for mouse oocyte meiotic maturation. Sci. Rep. 6, 30970.
Zhang, X., et al., 2006. Redox-induced apoptosis of human oocytes in resting follicles *in vitro*. J. Soc. Gynecol. Investig. 13, 451.
Zhang, Z., et al., 2017. Fluorene-9-bisphenol is anti-oestrogenic and may cause adverse pregnancy outcomes in mice. Nat. Commun. 8, 14585.
Zhu, C.C., et al., 2016. Toxic effects of HT-2 toxin on mouse oocytes and its possible mechanisms. Arch. Toxicol. 90, 1495–1505.
Zhu, X., et al., 2018. Effects of bisphenol A on ovarian follicular development and female germline stem cells. Arch. Toxicol. 92, 1–11.